

SUPPLEMENTARY MATERIAL

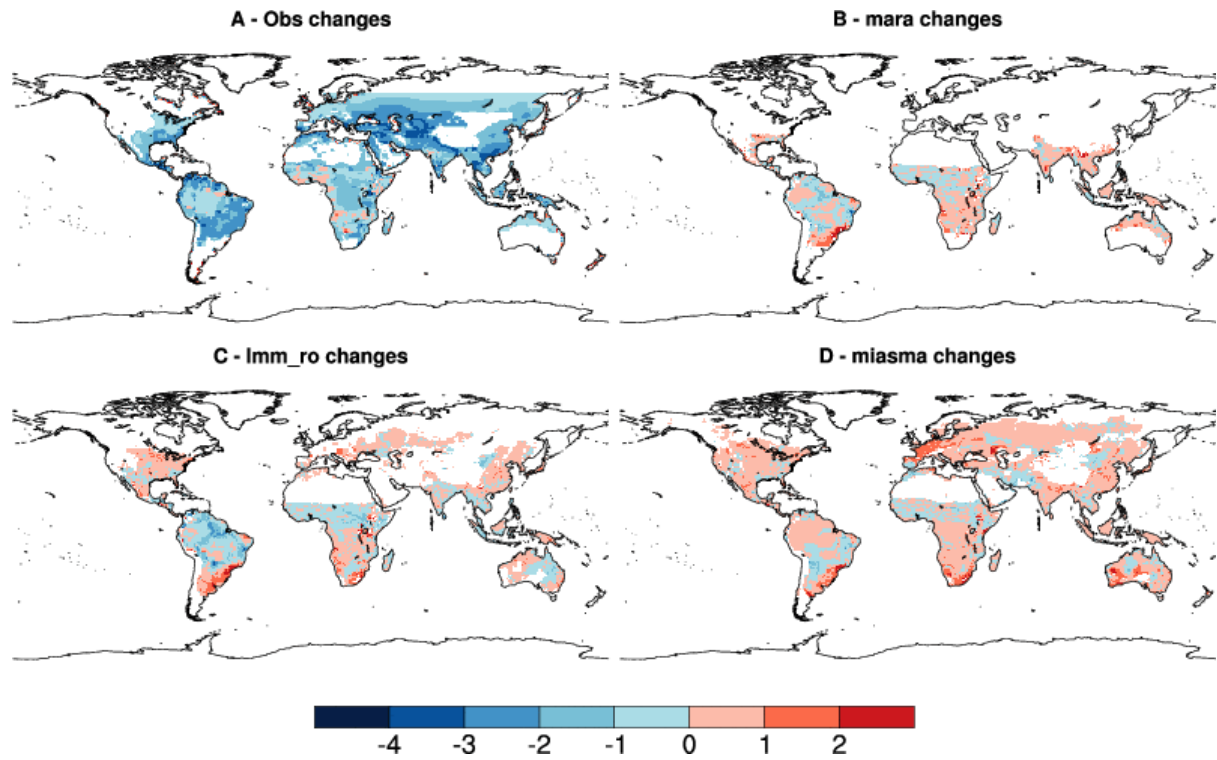


Figure S1: Change in endemicity class between 1900s and 2000s for the observations (A; based on Gething et al., 2010). For the simulations (B, C and D) changes in the length of the malaria transmission season are shown for only three malaria models (in months) driven by the CRUTS3.1 climate dataset.

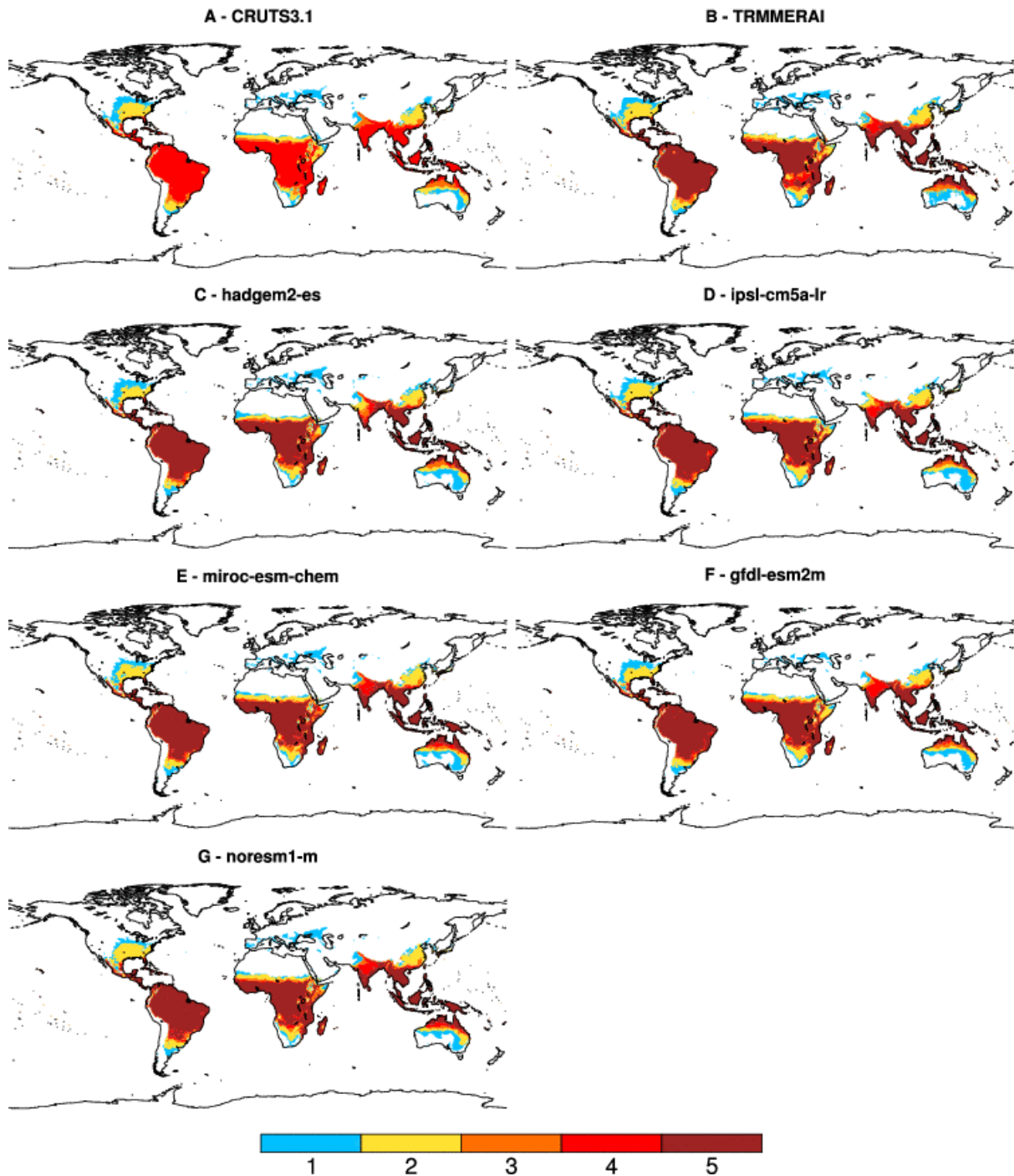


Figure S2. Estimation of current malaria distribution and validation.

The different colours show the number of malaria models which agree on the suitability of climate for malaria. This is carried out for two observation baseline (CRUTS3.1 over the period 1980-2009 & TRMMERAI over the period 1999-2010) and the historical experiments over the period 1980-2010 for the five different GCMs. Note that for the CRUTS3.1 baseline, only four malaria models were used (Imm_ro, miasma, mara & umea).

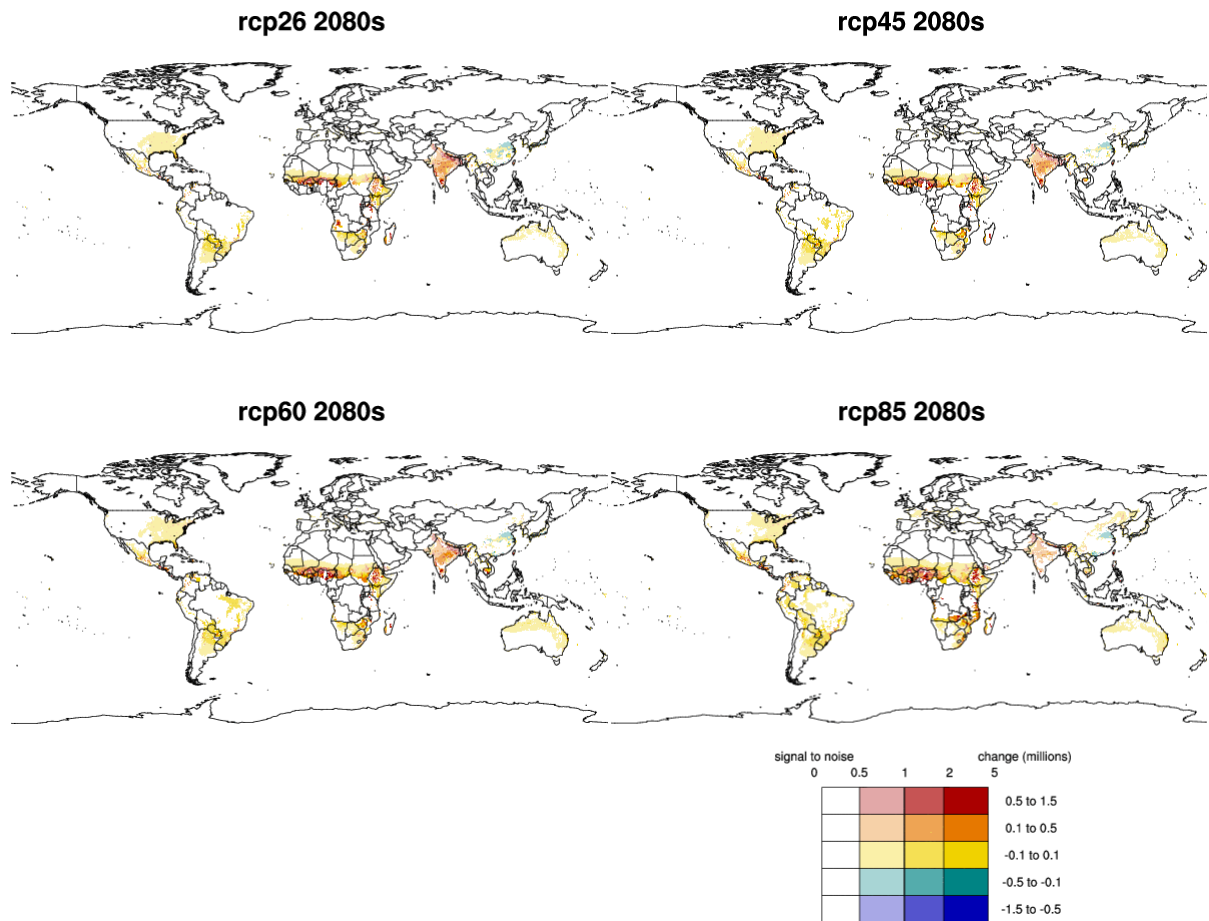
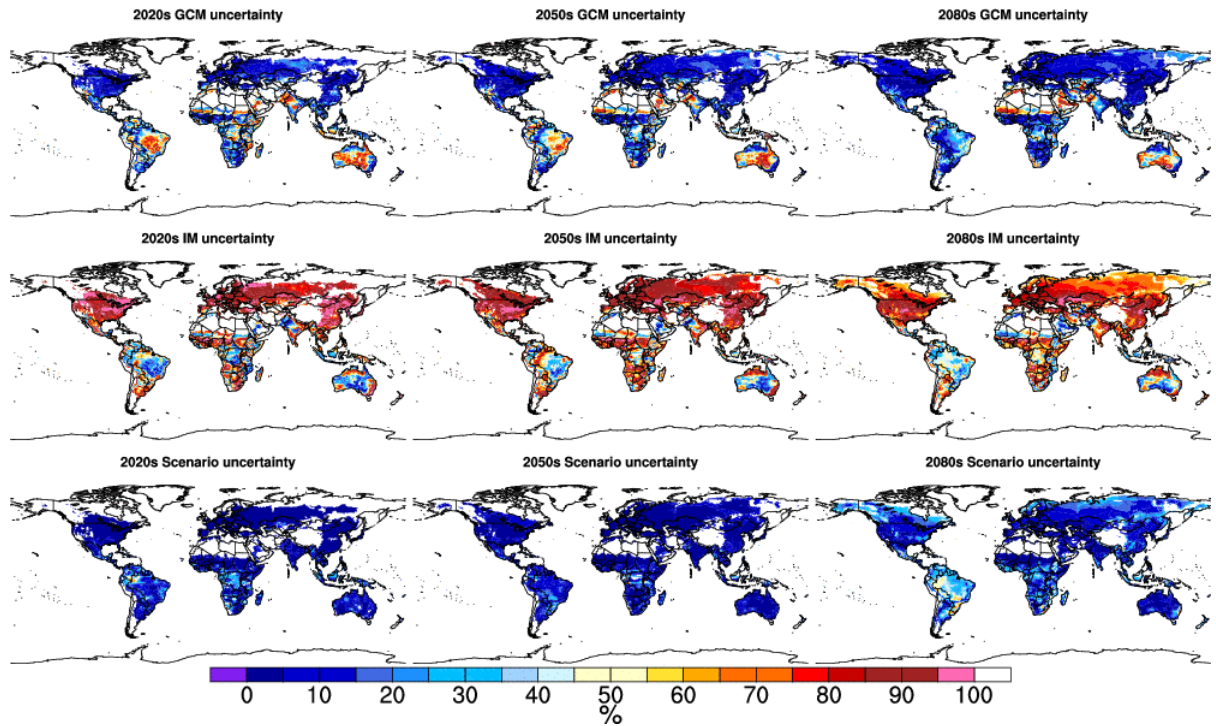


Figure S3. The effect of climate and population scenarios on the additional people at risk of malaria in the future (in millions). Each map shows the results for a different emission scenario (RCP). The different hues represent additional people at risk of malaria between 1980–2010 and 2069–2099 for the mean of CMIP5 sub-ensemble. The different saturations represent signal-to-noise (μ/Sigma) across the super ensemble (the noise is defined as one standard deviation within the multi-GCM and multi-malaria ensemble). The stippled area shows the multi-malaria model multi GCM agreement (60% of the models agree on the sign of changes).

Figure S4. Assessment of relative contribution of malaria impact model (MIM), climate model (GCM), and emissions scenario (RCP) to estimated future malaria distribution under climate change.



To estimate the various sources of uncertainty in the future scenarios we assumed a linear decomposition of the variance of the total uncertainty between three components (GCM/MIM/RCP). This is calculated for LTS future anomalies with respect to historical experiments:

$$\sigma_{TOT}^2 = \sigma_{GCM}^2 + \sigma_{MIM}^2 + \sigma_{RCP}^2$$

For a given time-slice, the variance of the parameter of interest (GCM for example) is calculated on the average (ensemble mean) across the other parameter dimensions (MIM and scenario) for each grid point:

$$GCM_{mean} = \frac{1}{N_{MIM} * N_{RCP}} * \sum_{MIM=1}^4 \sum_{RCP=1}^4 LTS_{anom}(MIM, RCP)$$

$$\sigma_{GCM}^2 = \frac{1}{N_{GCM}} * \sum_{GCM=1}^5 (GCM_{mean}(GCM) - \langle GCM_{mean}(GCM) \rangle)^2$$

We then show each component separately (as a percentage):

$$\sigma_{GCM}^2(\%) = 100 * \frac{\sigma_{GCM}^2}{\sigma_{TOT}^2}$$

Note that the linear assumption generally underestimates the total uncertainty.

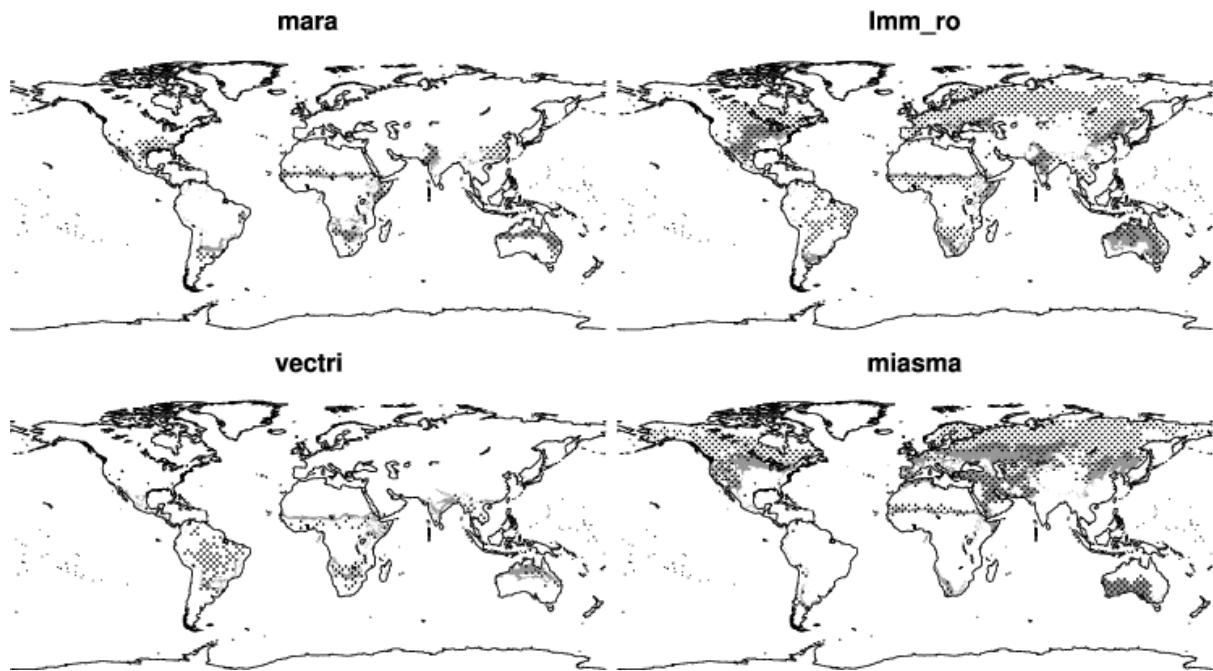
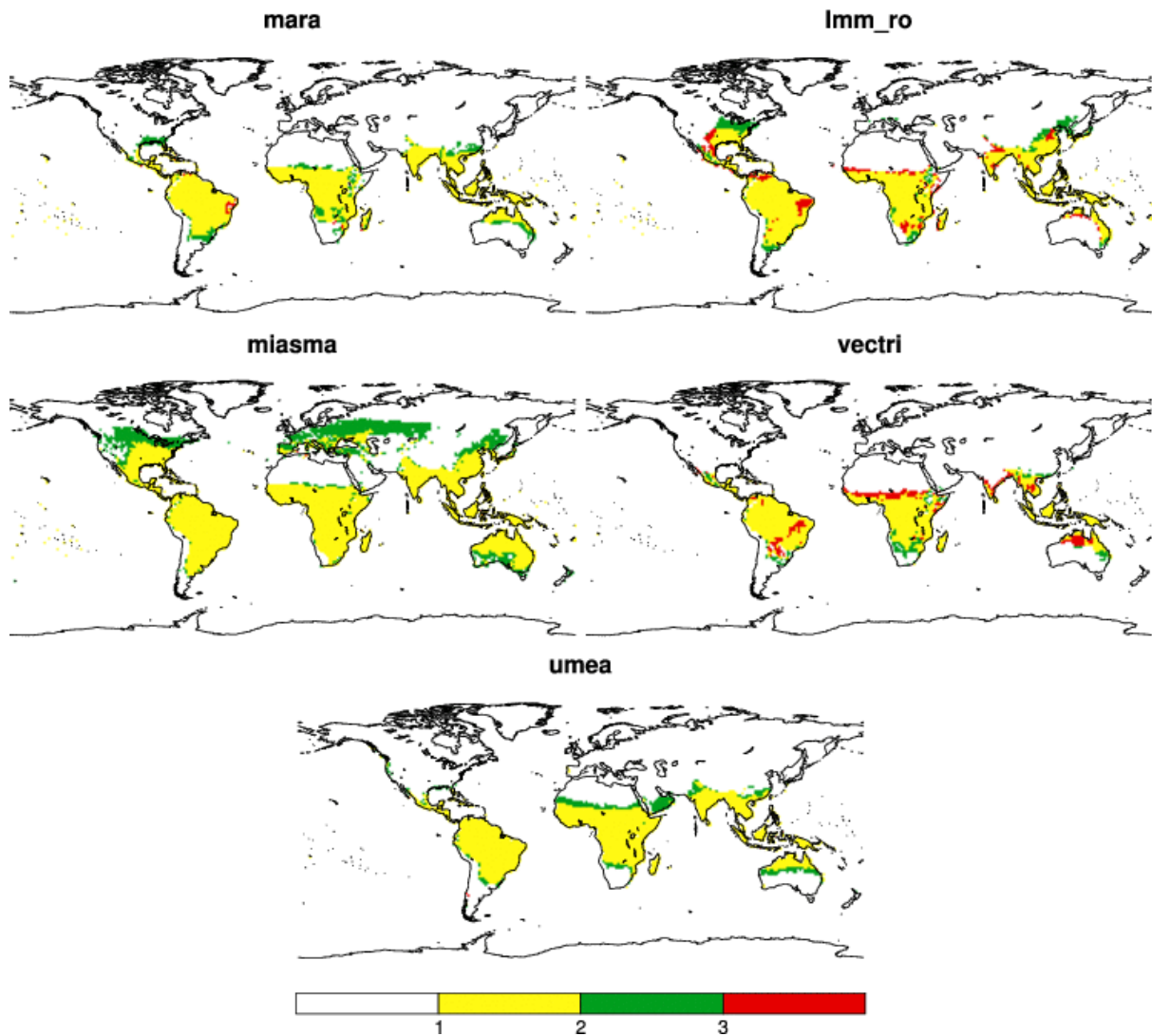


Figure S5: Sensitivity of the simulated malaria epidemic belt to climate change for the ISI-MIP ensemble. The gray shading depicts the location of the epidemic belt (for a short malaria transmission season e.g. $1 \text{ month} \leq \text{LTS} < 3 \text{ months}$) based on the multi-model ensemble mean for the historical experiments (1980-2010 average). The dotted area depicts the epidemic fringe location based on ensemble mean of the **rcp8.5 emission scenario for the 2080s** (most extreme climate change scenario).

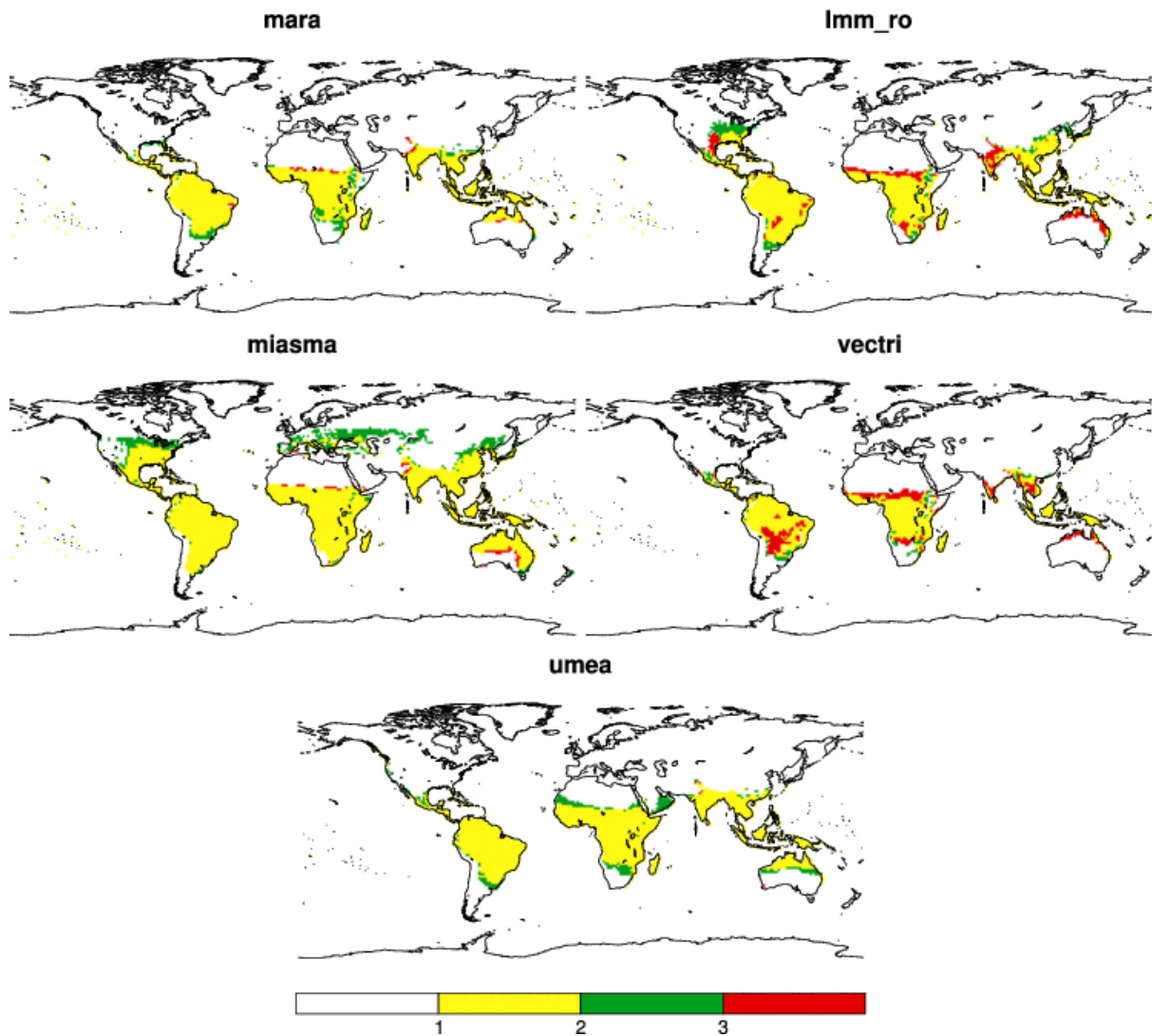


Future climate is still suitable for malaria transmission

Future climate becomes unsuitable for malaria transmission

Future climate becomes suitable for malaria transmission

Figure S6: Simulated changes in climate suitability for stable malaria transmission (CS) for the ISI-MIP noresm1 experiment. Changes are calculated for the most extreme emission scenario (rcp85) for the 2080s with respect to the historical run (1980-2010). White areas depict regions where future climate is still unsuitable for malaria, yellow where it is still suitable, red where it becomes unsuitable and green where it becomes suitable.

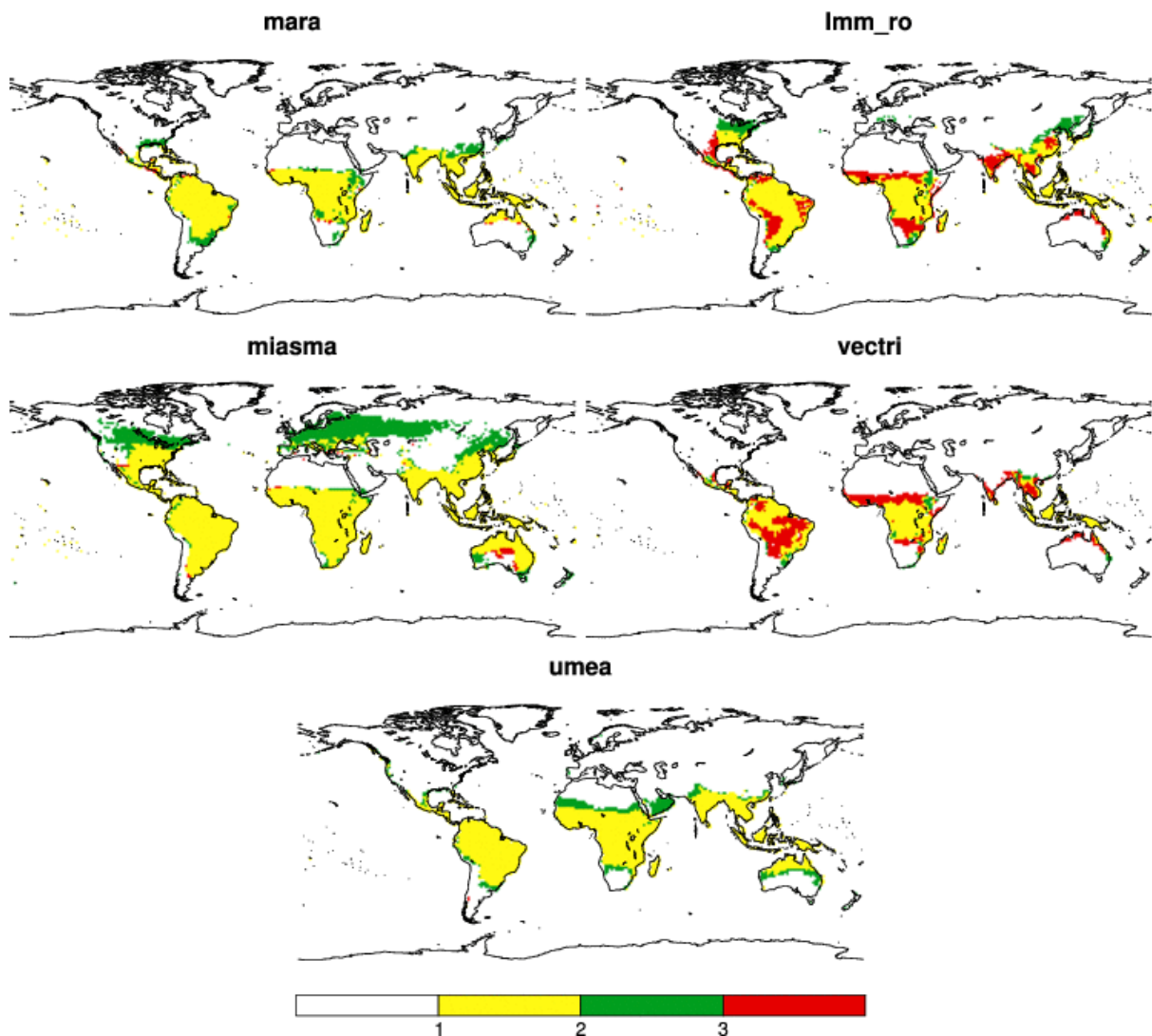


Future climate is still suitable for malaria transmission

Future climate becomes unsuitable for malaria transmission

Future climate becomes suitable for malaria transmission

Figure S7: Simulated changes in climate suitability for stable malaria transmission (CS) for the ISI-MIP gfdl_esm2m experiment. Changes are calculated for the most extreme emission scenario (rcp85) for the 2080s with respect to the historical run (1980-2010). White areas depict regions where future climate is still unsuitable for malaria, yellow where it is still suitable, red where it becomes unsuitable and green where it becomes suitable.

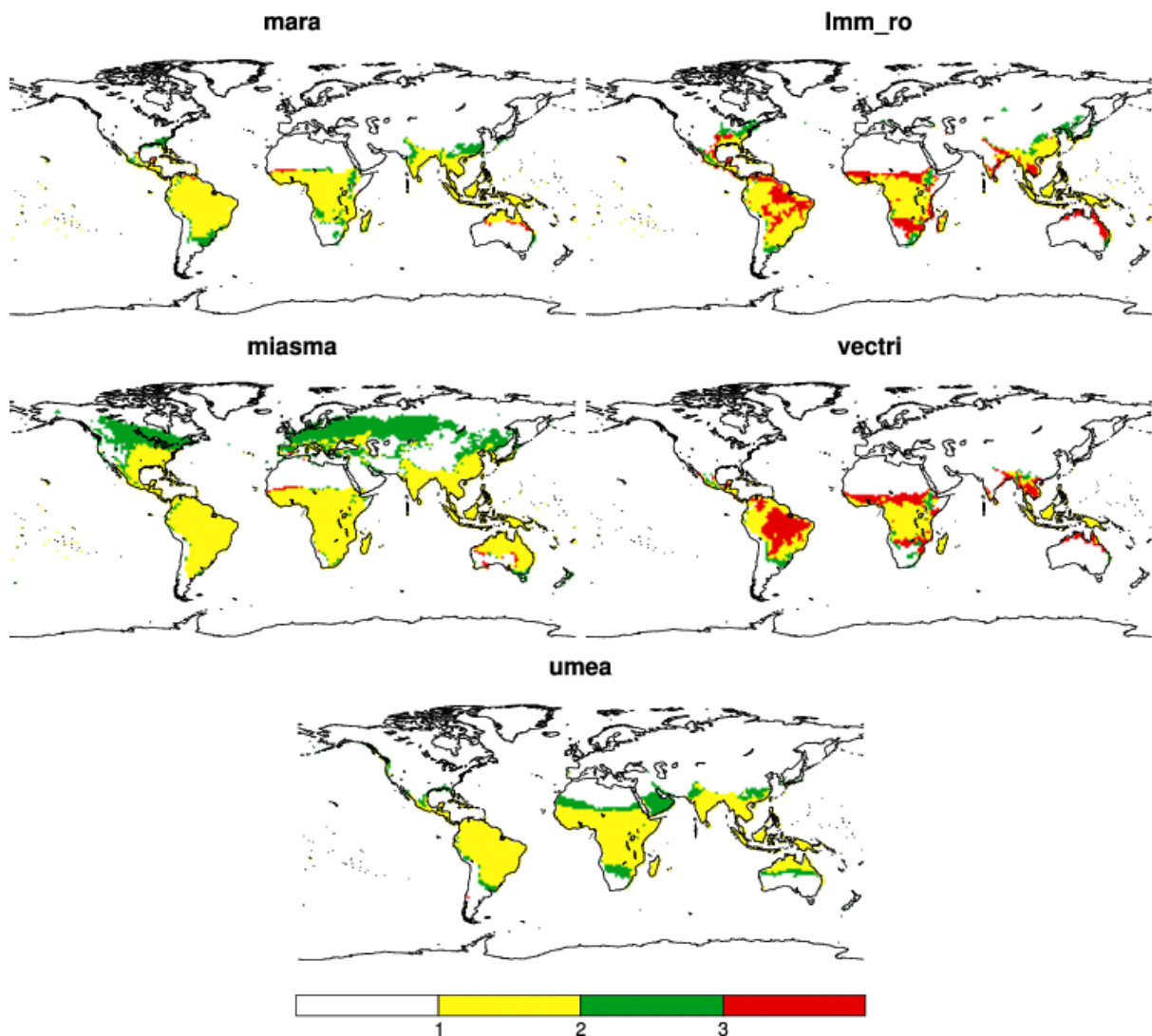


Future climate is still suitable for malaria transmission

Future climate becomes unsuitable for malaria transmission

Future climate becomes suitable for malaria transmission

Figure S8: Simulated changes in climate suitability for stable malaria transmission (CS) for the ISI-MIP ipsl-cm5a-lr experiment. Changes are calculated for the most extreme emission scenario (rcp85) for the 2080s with respect to the historical run (1980-2010). White areas depict regions where future climate is still unsuitable for malaria, yellow where it is still suitable, red where it becomes unsuitable and green where it becomes suitable.

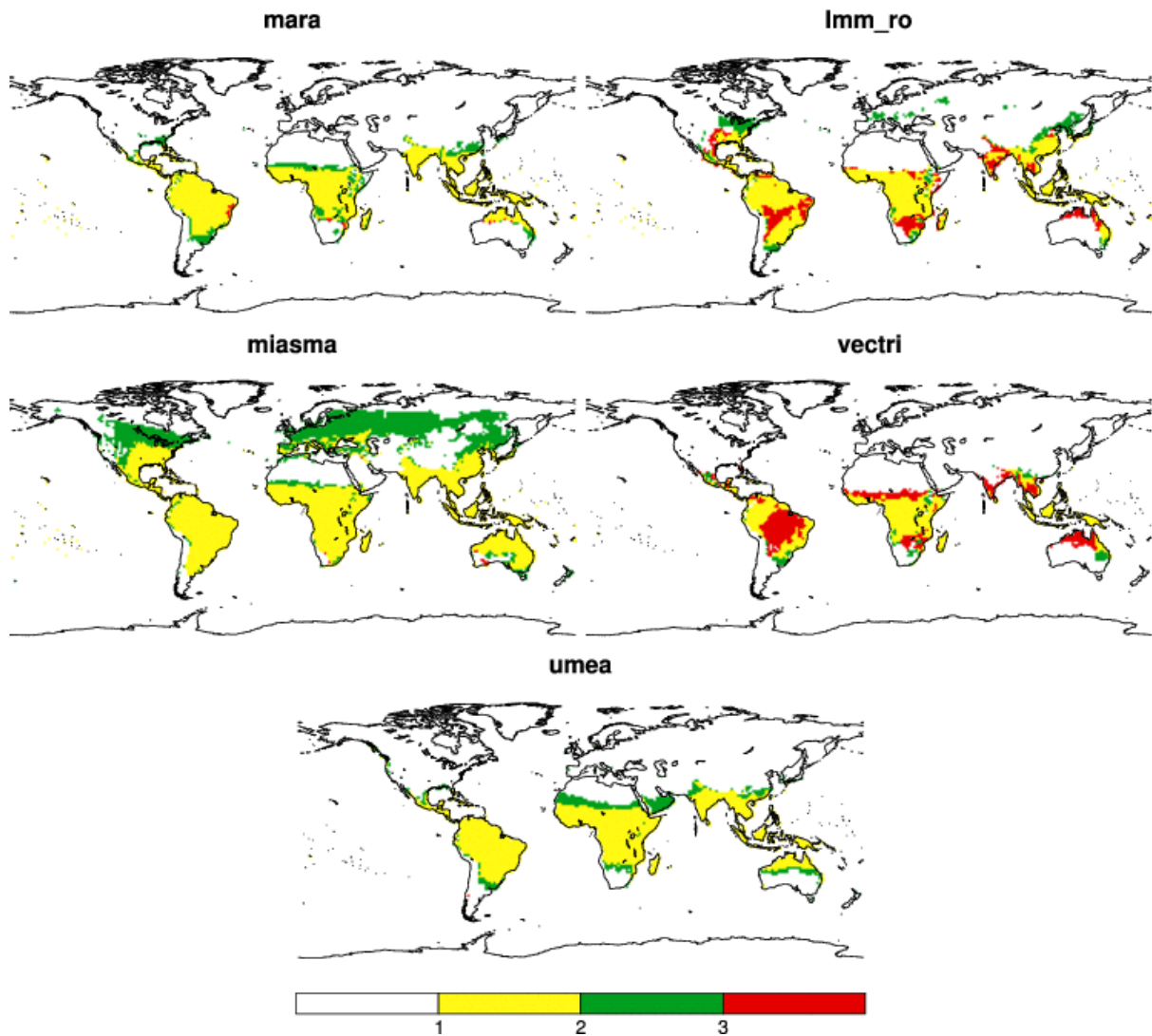


Future climate is still suitable for malaria transmission

Future climate becomes unsuitable for malaria transmission

Future climate becomes suitable for malaria transmission

Figure S9: Simulated changes in climate suitability for stable malaria transmission (CS) for the ISI-MIP hadgem2-es experiment. Changes are calculated for the most extreme emission scenario (rcp85) for the 2080s with respect to the historical run (1980-2010). White areas depict regions where future climate is still unsuitable for malaria, yellow where it is still suitable, red where it becomes unsuitable and green where it becomes suitable.



Future climate is still suitable for malaria transmission

Future climate becomes unsuitable for malaria transmission

Future climate becomes suitable for malaria transmission

Figure S10: Simulated changes in climate suitability for stable malaria transmission (CS) for the ISI-MIP miroc-esm-chem experiment. Changes are calculated for the most extreme emission scenario (rcp85) for the 2080s with respect to the historical run (1980-2010). White areas depict regions where future climate is still unsuitable for malaria, yellow where it is still suitable, red where it becomes unsuitable and green where it becomes suitable.

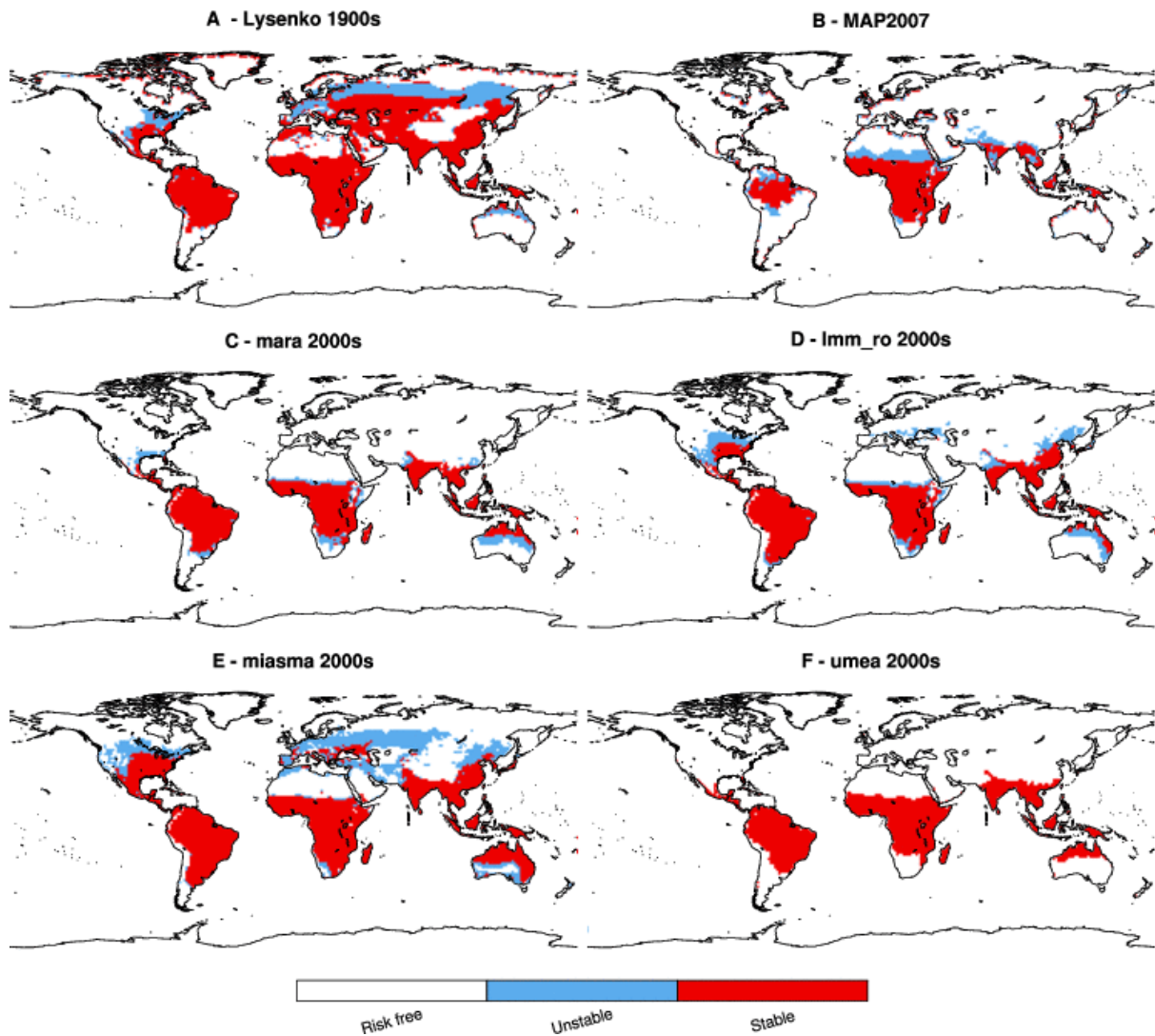


Figure S11. Observed (A and B) and simulated (C, D, E and F) malaria distribution (three categories, risk free in white, unstable/epidemic in blue, stable/endemic in red) for four malaria models. For the observation all endemic sub-categories (hypoendemic, mesoendemic, hyperendemic and holoendemic) have been included in the stable category. The 1900s data (A) is based on ref. 38 (considers all plasmodium infections), the 2000s (B) based on ref. 14 (considers only *P. falciparum* infections). For the simulations, unstable malaria is defined for a length of the transmission season (LTS) ranging between 1 and 3 months, suitable is defined for LTS above 3 months (based on CRUTS3.1 control runs for the period 1980-2009). For the UMEA malaria model only estimates of stable malaria were available.